25th ABCM International Congress of Mechanical Engineering
October 20-25, 2019, Uberlândia, MG, Brazil

COB-2019-0849
CONTINUOUS AND NUMERICAL SOLUTION FOR A TURBULENT TEMPORAL MIXING LAYER

Gabriel Marcos Magalhães
Jessica Guarato de Freitas Santos
Aristeu da Silveira Neto
Faculty of Mechanical Engeneering. Federal University of Uberlândia (UFU), Av. João Naves de Ávila 2121, 38400-902, Uberlândia-MG, Brazil
gabrielm@ufu.br, jessica.guarato@ufu.br, aristeus@ufu.br

Abstract. *The continuous solution and computational simulations are presented for a temporal mixing layer in the turbulent regime. To obtain the continuous solution it was applied the self-similar technique, and for the computational simulations, the MFSim code was used. The temporal mixing layer was simulated with Large Eddy Simulation (LES) and Unsteady Reynolds Averaged Navier-Stokes (URANS) models. The mean velocity profiles extracted from the computational simulations were compared with the profiles obtained by continuous solutions.*

Keywords: *temporal mixing layer, continuous solution, self similar solution, URANS, LES)*

1. INTRODUCTION

Free shear flows occur in the absence of walls and adverse pressure gradients. In these flows, spatial regions or temporal regions exist in which some properties profiles have similar shapes. In these regions, it is possible to transform all profiles into a single profile applying a function to the temporal or spatial profiles. This property is called self-similarity. In flows with a self-similar characteristic, it is possible to develop continuous solutions for certain properties of the flow.

A simple free shear flow to be modeled is the temporal mixing layer. Two streams with different velocities (U_1 and U_2) define and maintain the flow. The temporal mixing layer is presented in many applications like combustion (Bellan, 2017), evaporation (Okong'o and Bellan, 2004) and particulate dispersion (Ling *et al.*, 1998).

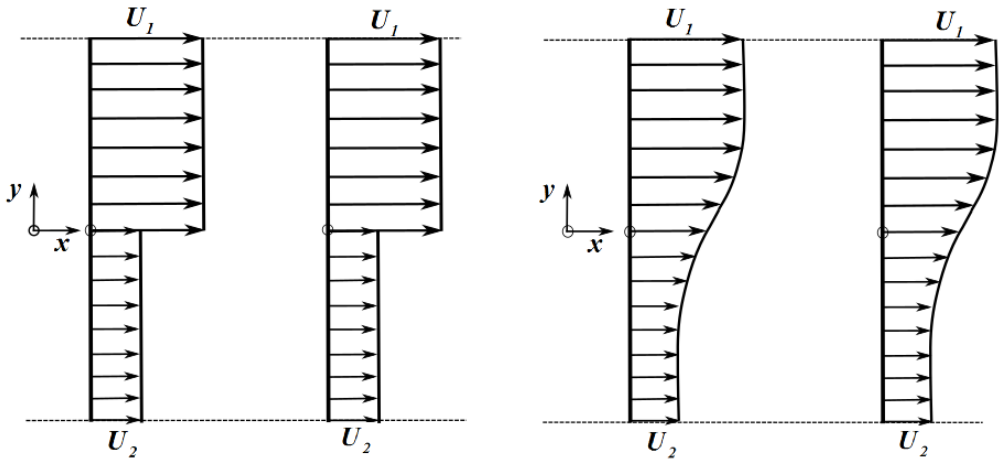

(a) (b)

Figure 1: Temporal mixing layer at (a) $t = 0\,s$ and (b) $t > 0\,s$.

At an initial time, $t = 0$ s, the velocity field presents an infinite gradient in the center of the domain. At this time the thickness of the shear layer is $\delta(t = 0) = 0$ (Fig. 1(a)). With the time development, the linear momentum diffusion process attenuates this gradient, generating a velocity profile characterized by an inflection point (Fig. 1(b)). In the laminar regime, the diffusion occurs by the molecular movement. In the turbulent regime, the vortex structures will accelerate this

process of molecular diffusion in orders of magnitude by increasing the local gradients and the number of gradients per unit volume.

The transition of the mixing layer under temporal development has some important characteristics to be observed. If the flow occurs in the absence of any perturbation, it will remain in the laminar regime diffusing the information, but without transitioning. The transition process starts if some perturbation is inserted into the flow, leading to the fully turbulent regime. According to the linear stability theory (Betchov and Szewczyk, 1963), a temporal mixing layer becomes unstable, if it is disturbed even for Reynolds numbers tending to zero.

The objective with the continuous solution is not to model Kelvin-Helmholtz instabilities, but only to model the average flow. As shown in Figs. 1(a) and 1(b), the evolution of the flow occurs only in y-direction and time. Since there is no spatial variation in x-direction at any time, the development is temporal even though there is variation in y. It is possible to observe that the velocity profiles, shown in Figs. 1(a) and 1(b), are self-similar. The self-similar behavior allows the self-similarity theory to be used for the solution of the differential model.

2. METHODOLOGY

The present work has two distinct parts: the continuous solution and the computational simulations. In the first subsection, the methodology to obtain a continuous solution is presented. Then, the procedure and parameters for the computational simulations are presented.

2.1 Exact solution

The differential mathematical model for the turbulent temporal mixing layer is composed of the linear momentum balance and mass balance equations. Some hypotheses and considerations are assumed for the simplification of the complete equations.

The first assumption is to consider the process of diffusive transport, promoted by turbulence, orders of magnitude larger than the molecular diffusive process. Thus, the molecular diffusion term is not included in the final equation.

According to the physical nature of the temporal mixing layer, the average flow occurs in the x-direction and only depends on y-direction and time t. With this assumption, it is possible to simplify the advective term. Therefore, the filtered Navier-Stokes equation for x-direction results in

$$\frac{\partial \bar{u}(y,t)}{\partial t} = \frac{\partial \tau_{xy}}{\partial y}, \tag{1}$$

where $\bar{u}(y,t)$ is the mean x-velocity and τ_{xy} is a component of the Boussinesq-Reynolds tensor.

Using the turbulent viscosity hypothesis and the Boussinesq-Prandtl's mixing length model, the τ_{xy} component of the Boussinesq-Reynolds tensor can be modeled as follows:

$$\tau_{xy} = \nu_t \frac{\partial \bar{u}}{\partial y} = l_m^2 \left|\frac{\partial \bar{u}}{\partial y}\right| \frac{\partial \bar{u}}{\partial y}, \tag{2}$$

where ν_t is the turbulent kinematic viscosity, and l_m is an empirical parameter of the model that is estimated by experiments and can be changed according to the flow.

Considering $\left|\frac{\partial \bar{u}}{\partial y}\right| \geq 0$ and, in the temporal mixing layer, $\frac{\partial \bar{u}}{\partial y} \geq 0$ for every y, then $\left|\frac{\partial \bar{u}}{\partial y}\right| = \frac{\partial \bar{u}}{\partial y}$. Substituting Eq. (2) in (1), it is obtained that

$$\frac{\partial \bar{u}}{\partial t} = l_m^2 \frac{\partial}{\partial y}\left[\left(\frac{\partial \bar{u}}{\partial y}\right)^2\right], \tag{3}$$

where $l_m = \alpha\,\delta(t)$. The coefficient α must be determined experimentally, either by material experiment or by computational simulation via DNS (Direct Numerical Simulation). An analysis of this constant will be presented in the results section. The $\delta(t)$ is the length of the diffusion zone.

The initial and boundary conditions of the problem are given by:

$$\bar{u}(y, t=0) = \bar{u}_o(y), \tag{4a}$$

$$\bar{u}\left(y = \frac{\delta(t)}{2}\right) = U_1, \tag{4b}$$

$$\frac{\partial \bar{u}}{\partial y}\left(y = \frac{\delta(t)}{2}\right) = 0, \tag{4c}$$

$$\bar{u}(y=0, t) = \bar{U}, \tag{4d}$$

where $\bar{u}_o(y)$ is the inicial field of x-velocity and $\bar{U} = \dfrac{U_1 + U_2}{2}$.

In the transformation of Eq. (3) through the self-similarity theory, a self-similar variable (η) and a self-similar function $F(\eta)$ are used and given by:

$$\eta(y,t) = \frac{y}{\delta(t)}, \tag{5}$$

and

$$\frac{\bar{u}(y,t) - \bar{U}}{\tilde{U}} = F(\eta), \tag{6}$$

in which $\tilde{U} = \dfrac{U_1 - U_2}{2}$.

Taking the derivatives in time and space of the self-similarity function, and substituting them in Eq. (3), it is determined that

$$F'F'' + \underbrace{\frac{1}{2\,\tilde{U}\alpha^2}\frac{d\delta}{dt}}_{a_{ot}}\eta F' = 0, \tag{7}$$

where the a_{ot} term must be a constant, since the solution of this differential equation must result in a function dependent only on η. Thereby,

$$\frac{1}{2\,\tilde{U}\alpha^2}\frac{d\delta}{dt} = a_{ot} \longrightarrow \delta(t) = 2\,\tilde{U}\alpha^2 a_{ot}\,t \longrightarrow \delta(t) = K_t\,t, \tag{8}$$

where $K_t = 2\,\tilde{U}\alpha^2 a_{ot}$ is a constant relative to the turbulent flow, which can be determined by using a boundary condition. To obtain Eq. (8), it was necessary to determine the value for an integration constant. The initial condition $\delta(t=0) = 0$ was used to calculate the value of this constant.

The ordinary differential model needs some boundary conditions for Eq. (7). These boundary conditions are given by

$$F\left(\eta = \frac{1}{2}\right) = 1, \tag{9a}$$

$$F'\left(\eta = \frac{1}{2}\right) = 0, \tag{9b}$$

$$F\left(\eta = 0\right) = 0. \tag{9c}$$

Equations (7) and (9) compose the complete ordinary differential model, which admits an analytical solution, as will be presented next. Equation (7) can be rewritten as

$$F'(F'' + a_{ot}\eta) = 0, \tag{10}$$

allowing its decomposition into two equations. The first equation is given by

$$F' = 0, \tag{11}$$

and leads to a trivial solution $F(\eta) = cte$. The second equation is given by

$$F'' + a_{ot}\eta = 0, \tag{12}$$

and its result is obtained by the method of separation of variables followed by integration of both sides of the equation:

$$F(\eta) = -\frac{a_{ot}}{6}\eta^3 + c_{1t}\eta + c_{2t}, \tag{13}$$

in which $a_{ot} = \dfrac{K_t}{2\alpha^2\tilde{U}}$, and c_{1t} and c_{2t} are integration constants.

Using the boundary condition given by Eq. (9c), $F(0) = 0$, it is obtained that $c_{2t} = 0$. The other two boundary conditions, given by Eqs. (9a) and (9b), provide $a_{ot} = 24$ and $c_{1t} = 3$. Thus, it is implied that the function $F(\eta)$ is given by

$$F(\eta) = -4\eta^3 + 3\eta. \tag{14}$$

Returning to the a_{ot} constant, already in possession of its determined value, it is implied that

$$a_{ot} = \frac{K_t}{2\,\alpha^2\,\tilde{U}} = 24 \longrightarrow K_t = 48\,\alpha^2\,\tilde{U}, \tag{15}$$

therefore, substituting Eq. (15) in (8), it is found that

$$\delta(t) = K_t\,t = 48\,\alpha^2\,\frac{(U_1 - U_2)}{2}\,t \longrightarrow \delta(t) = 24\,\alpha^2\,(U_1 - U_2)\,t. \tag{16}$$

In the solution presented in Eq. (17), it was not considered the mixing length at initial time. If the mixing length begin with a non-zero mixing length, the correct equation is

$$\delta(t) = \delta_o + 24\,\alpha^2\,(U_1 - U_2)\,t, \tag{17}$$

where δ_o is the initial mixing length.

Finally, it is obtained from Eqs. (5), (6) and (14) that

$$\bar{u}(\eta) = \bar{U} + \tilde{U}\,(3\eta - 4\eta^3), \tag{18}$$

or

$$\bar{u}(\eta) = \bar{U} + \tilde{U}\,\left[3\left(\frac{y}{\delta(t)}\right) - 4\left(\frac{y}{\delta(t)}\right)^3\right]. \tag{19}$$

2.2 Computational simulations

Four computational simulations were made for the present work. All of these simulations were performed using the MFSim code. The MFSim is an "in-house" code developed in the Laboratory of Fluid Mechanics (MFLab) from the Federal University of Uberlandia (UFU). The base of the MFSim is an adaptive block-structured regular and cartesian mesh which reduces the computational cost. To treat the turbulence, in this code the Large Eddy Simulation (LES) models and Unsteady Reynolds Average Navier-Stokes (URANS) models are available to the user. It is possible to simulate problems like fluid-structure interaction, multiphase flows, reactive and turbulent flows considering 3D domains and parallel processing using MFSim (Neto *et al.*, 2019; Melo *et al.*, 2018; Gasche *et al.*, 2012; Denner *et al.*, 2014).

The first simulation was performed using the LES (Large Eddy Simulation) methodology with Germano's dynamic model (Germano *et al.*, 1991). A uniform mesh of $512 \times 256 \times 512$ elements were used in a domain of $8[m] \times 4[m] \times 8[m]$. A fluid with $\nu = 0.01$ m^2/s in two streams with velocities of 20 m/s and -20 m/s was used. The velocity profiles at specific times were obtained with equally spaced probes. To treat the obtained data, it was employed a spatial averaging process.

For the other simulations, three URANS models were used: the standard $k - \epsilon$ model proposed by Jones and Launder (1972), the realizable $k - \epsilon$ model of Shih *et al.* (1995) and the $k - \omega$ model proposed by Wilcox *et al.* (1993). The standard $k - \epsilon$ and the realizable $k - \epsilon$ models were implemented in the MFSim as part of the present work.

All simulations with URANS models used the same setup. Therefore, a domain of $8[m] \times 4[m] \times 0,0625[m]$ was defined with a uniform mesh of $128 \times 64 \times 1$ cells. The molecular properties of the fluid and stream velocities used in these simulations were the same as presented for the first simulation.

The computational simulation of the turbulent temporal mixing layer requires an initial perturbation to promote the turbulent transition. In the LES simulation, it was used a volumetric perturbation applying $10\,\%$ of white noise in each direction. For URANS computational simulations, the perturbation is inserted as a turbulent intensity that varies according to the flow. In the computational simulations performed using MFSim code, it was employed $0.5\,\%$ of turbulent intensity for all models.

3. PRELIMINARY RESULTS

The results can be divided in three parts: the results of the computational simulation using a LES model, an analysis for the value of the constant α, that compounds the continuous solution, and the results of the computational simulations considering URANS models.

3.1 Results of LES simulation

The LES simulation was performed in MFSim code using the dynamic Smagorinsky model. When LES models are used, the computational domain must be three-dimensional. It is possible to obtain a detailed instantaneous velocity field. The turbulent structures at $t = 0.17$ s can be visualized using a Q criteria (Q = 0.1) presented by the x-velocity magnitude. A perspective view (Fig. 2(a)) and a top view (Fig. 2(b)) are shown.

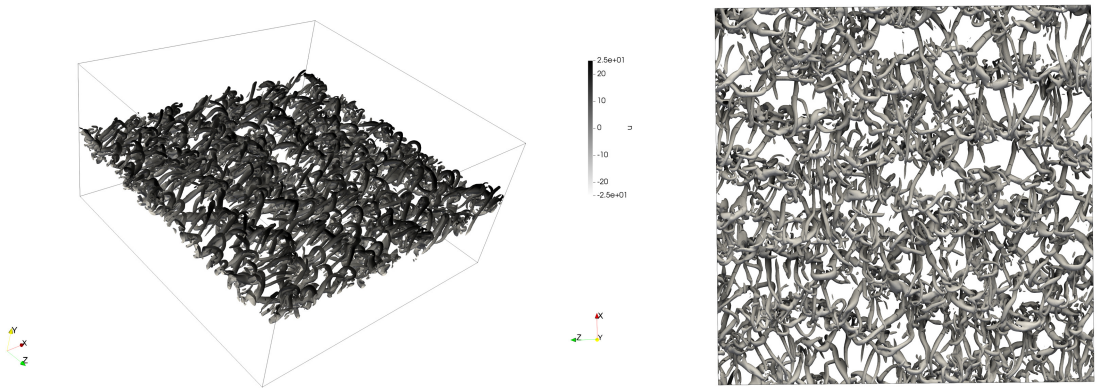

(a) (b)

Figure 2: Q criteria (Q = 0.1) for a turbulent temporal mixing layer at $t = 0.17$ s.

It is possible to observe interactions between the turbulent structures in all directions. For this reason, a spatial average is necessary to obtain the mean x-velocity profile. Equally spaced probes were used and the spatial average was applied to obtain instantaneous profiles.

Silvestrini (2000) showed an analysis in which he concluded that is possible to link results for spatial mixing layers and temporal mixing layers in the self-similar region. Because of that, it is possible to compare the results with the experimental work of Bell and Mehta (1990), who experimented a turbulent spatial mixing layer. The results of the computational simulation using a LES model were compared with the self-similar profile by the continuous solution and with the experimental data. The results of the computational simulation were compared at $t = 0.1206$ s, $t = 0.1336$ s, $t = 0.146$ s, $t = 0.15$ s, $t = 0.17$ s and $t = 0.2$ s. This comparison is exhibited in Fig. 3.

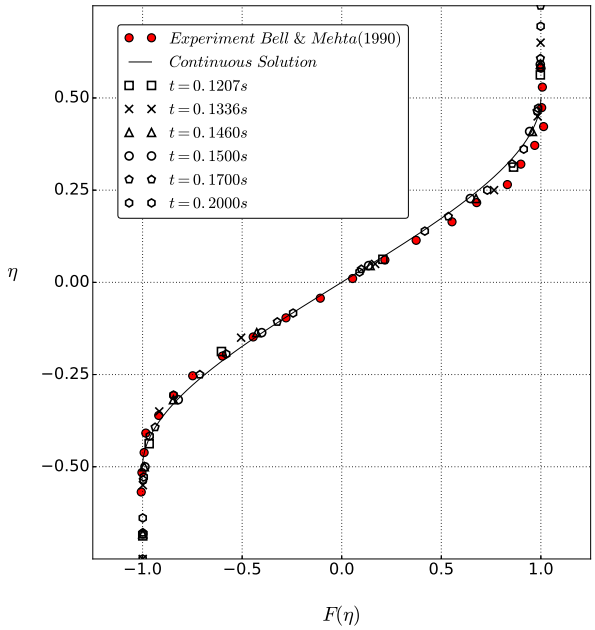

Figure 3: Comparison of the self-similar profile $F(\eta)$ between experimental results of Bell and Mehta (1990), the continuous solution and results of LES computational simulation with MFSim.

In Fig. 3, it is possible to observe a good agreement between the continuous solution and experimental data. It is also possible to notice that the results obtained by computational simulation presented a good agreement with the continuous solution and, hence, with experimental results of Bell and Mehta (1990) for all analyzed times.

3.2 The influence of the choosen value for α

The constant α is presented in the solution for the mixing length (δ) given by the Eq. (17) and, consequently, in η (Eq. (5)) and $\bar{u}(y,t)$ (Eq. (19)). All of the continuous solutions for a temporal mixing layer can be affected by the value of constant α, which is an empirical value.

According to Wilcox *et al.* (1993), the value for a spatial mixing layer is $\alpha = 0.07$, based in experimental observations. As it is possible to link results for spatial mixing layers and temporal mixing layers in the self-similar region, $\alpha = 0.07$ can be a good choice for the temporal mixing layer. In the present work, the continuous solution for $\delta(t)$ using $\alpha = 0.07$ and $\alpha = 0.06$ was compared with LES data from Silvestrini (2000). The results are shown in Fig. 4. and they are dependent on the non-dimensional time τ^*.

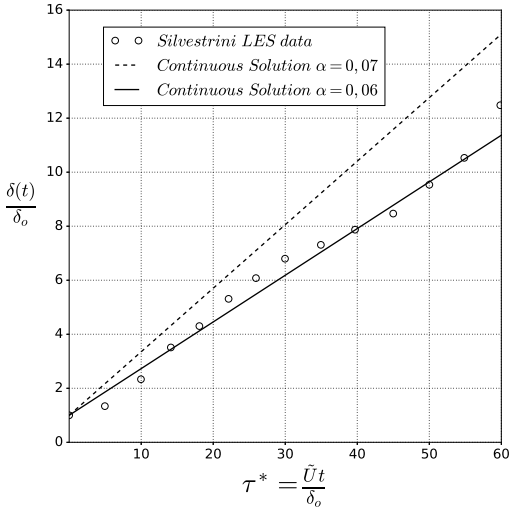

Figure 4: Comparison between the normalized mixing length obtained by Silvestrini, through LES simulation, and the value obtained by Eq. (17) considering $\alpha = 0.06$ and $\alpha = 0.07$.

It is possible to conclude observing Fig. 4 that the solution for $\alpha = 0.06$ presented a better agreement with Silvestrini LES data than the solution for $\alpha = 0.07$. An important remark is the interval of comparison, because $\tau^* = 60$ can be somewhat time-dependent of the stream velocity values. Therefore, the continuous solution for the velocity profiles was compared with the data obtained with the MFSim code considering LES for $\tau^* = 77.25$ and $\tau^* = 108.8$. The comparisons are shown in Fig 5(a) for $\tau^* = 77.25$ and in Fig 5(b) for $\tau^* = 108.8$.

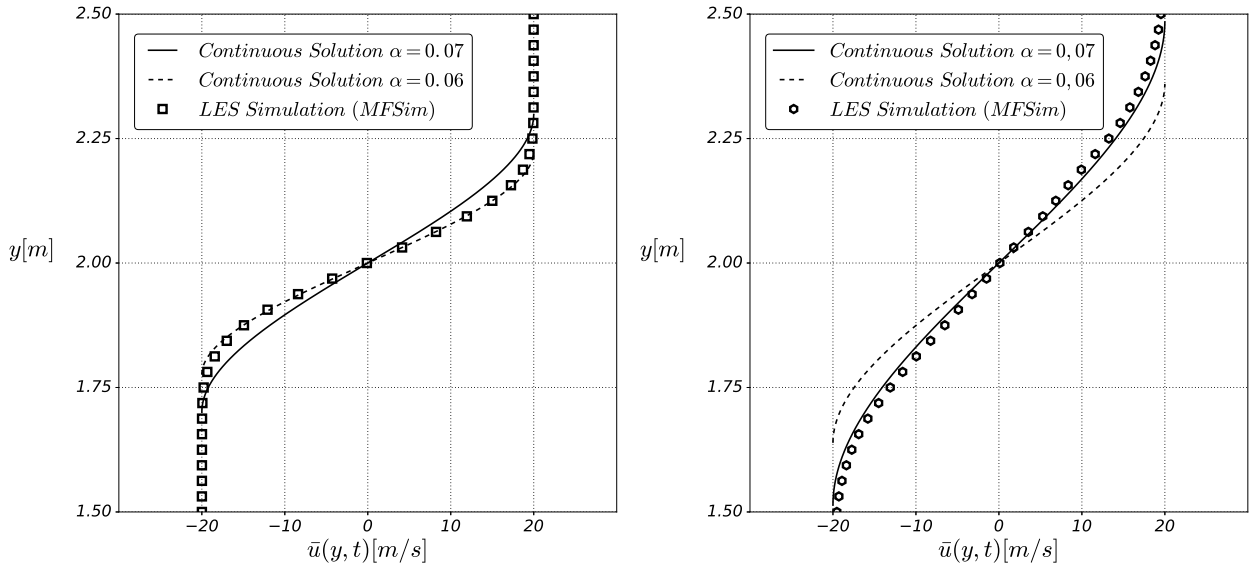

Figure 5: Continuous solution for $\bar{u}(y,t)$ using $\alpha = 0.06$ and $\alpha = 0.07$ compared with LES simulation results from MFSim code for (a) $\tau^* = 77.25$ and (b) $\tau^* = 108.8$.

Analyzing Fig. 5(a), for $\tau^* = 77.25$, it is possible to conclude that the continuous solution considering $\alpha = 0.06$ presented a better agreement with the data extracted from the LES simulation using MFSim code than the continuous solution adopting $\alpha = 0.07$. However, for $\tau^* = 108.8$ (Fig. 5(b)), the best agreement of the computational simulation results was with the continuous solution using $\alpha = 0.07$. This behavior evidenced that an ideal situation would be a

dynamic evaluation of the value of α. It is possible to adjust a time-dependent expression for α using results of the computational simulations and continuous solution for $\delta(t)$ or $\bar{u}(y,t)$.

3.3 Results of URANS simulations

As previously reported, simulations of a turbulent temporal mixing layer in the MFSim code were performed using three URANS models: the standard $k-\omega$ model, the realizable $k-\epsilon$ model, and the standard $k-\epsilon$ model. The results of the computational simulations using URANS were compared with the result of the MFSim simulation using LES, and also with the continuous solution profile at t = 0.15 s. This comparison is shown in Fig. 6.

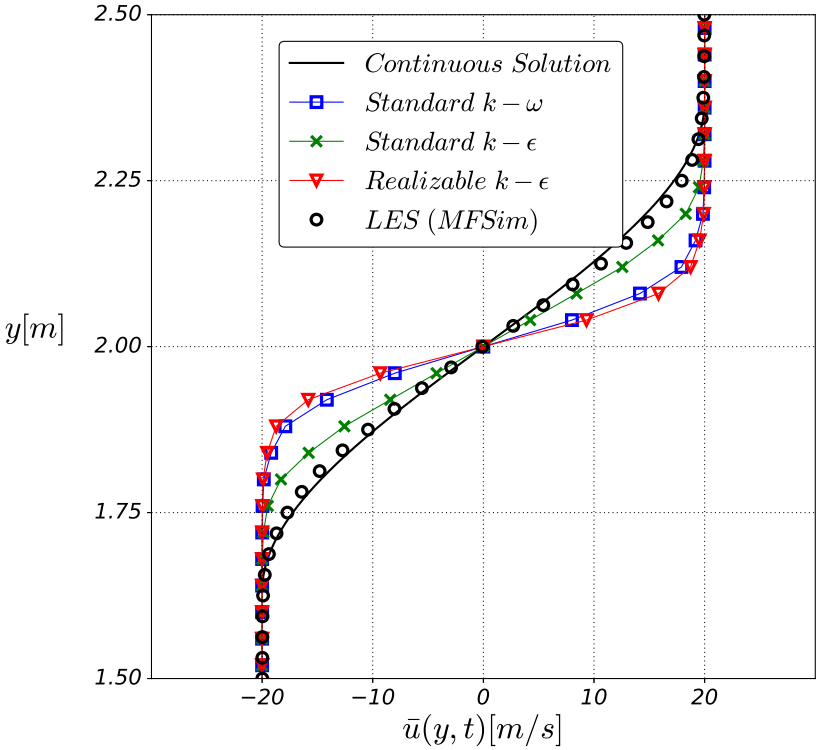

Figure 6: Comparison of the mean x-velocity profile $\bar{u}(y,t)$ obtained using URANS models, LES model and the continuous solution.

The realizable $k-\epsilon$ model and the standard $k-\omega$ model did not presented results close to the continuous solution profile of $\bar{u}(y,t)$. The standard $k-\omega$ model is indicated to simulate low Reynolds number flows, and the simulated temporal mixing layer does not have this characteristic. The realizable $k-\epsilon$ model was idealized for flows that have complex modeling effects such as curvature effects or adverse pressure gradients, that is not the case of the temporal mixing layer, which is a free shear flow.

The standard $k-\epsilon$ model is suitable for free shear flows with high Reynolds numbers, such as the turbulent temporal mixing layer. So, this is the most adequate turbulence model to simulate the considered type of flow. The results of the standard $k-\epsilon$ model presented the best agreement with the LES simulation results, and with the continuous solution for $\bar{u}(y,t)$.

4. CONCLUSIONS

Continuous solutions for the mixing length $\delta(t)$ and the mean x-velocity profile $\bar{u}(y,t)$ of a turbulent temporal mixing layer were developed. The velocity profile were compared with experimental data and with numerical results performed with the MFSim code. The continuous solutions presented a good agreement with these results, but it was possible to observe that the value of the constant α can modify all continuous profiles.

The computational simulation using LES presented better agreement with the continuous solution for $\bar{u}(y,t)$ than the results obtained using URANS models. Despite the better performance, the computational cost of a LES simulation is greater than a simulation using URANS models.

It is important to emphasize that the computational simulations do not use the continuous solutions at any moment, and the continuous solutions are not dependent of any data provided by the computational simulations. Therefore, the continuous solutions can be used as an interesting tool for comparison of results and validation of computational codes.

5. ACKNOWLEDGEMENTS

The authors acknowledge CAPES, Petrobras, CNPq and FAPEMIG for their support of this work.

6. REFERENCES

Bell, J.H. and Mehta, R.D., 1990. "Development of a two-stream mixing layer from tripped and untripped boundary layers". *AIAA journal*, Vol. 28, No. 12, pp. 2034–2042. doi:10.2514/3.10519.

Bellan, J., 2017. "Direct numerical simulation of a high-pressure turbulent reacting temporal mixing layer". *Combustion and Flame*, Vol. 176, pp. 245–262.

Betchov, R. and Szewczyk, A., 1963. "Stability of a shear layer between parallel streams". *The Physics of Fluids*, Vol. 6, No. 10, pp. 1391–1396. URL `https://doi.org/10.1063/1.1710959`.

Denner, F., van der Heul, D.R., Oud, G.T., Villar, M.M., da Silveira Neto, A. and van Wachem, B.G., 2014. "Comparative study of mass-conserving interface capturing frameworks for two-phase flows with surface tension". *International Journal of Multiphase Flow*, Vol. 61, pp. 37–47.

Gasche, J.L., Barbi, F. and Villar, M.M., 2012. "An efficient immersed boundary method for solving the unsteady flow through actual geometries of reed valves".

Germano, M., Piomelli, U., Moin, P. and Cabot, W.H., 1991. "A dynamic subgrid-scale eddy viscosity model". *Physics of Fluids A*, Vol. 3, No. 7.

Jones, A. and Launder, D., 1972. "Lectures in mathematical models of turbulence".

Ling, W., Chung, J., Troutt, T. and Crowe, C., 1998. "Direct numerical simulation of a three-dimensional temporal mixing layer with particle dispersion". *Journal of Fluid Mechanics*, Vol. 358, pp. 61–85.

Melo, R., Kinoshita, D., Villar, M., Serfaty, R. and Silveira-Neto, A., 2018. "Simulation of thermal transfer using the immersed boundary method and adaptive mesh". In *ICHMT DIGITAL LIBRARY ONLINE*. Begel House Inc.

Neto, H.R., Cavalini, A., Vedovoto, J., Neto, A.S. and Rade, D., 2019. "Influence of seabed proximity on the vibration responses of a pipeline accounting for fluid-structure interaction". *Mechanical Systems and Signal Processing*, Vol. 114, pp. 224–238.

Okong'o, N.A. and Bellan, J., 2004. "Consistent large-eddy simulation of a temporal mixing layer laden with evaporating drops. part 1. direct numerical simulation, formulation and a priori analysis". *Journal of Fluid Mechanics*, Vol. 499, pp. 1–47.

Shih, T.H., Liou, W.W., Shabbir, A., Yang, Z. and Zhu, J., 1995. "A new k-ϵ eddy viscosity model for high reynolds number turbulent flows". *Computers & Fluids*, Vol. 24, No. 3, pp. 227–238.

Silvestrini, J.H., 2000. "Dynamics of coherent vortices in mixing layers using direct numerical and large-eddy simulations". *Journal of the Brazilian Society of Mechanical Sciences*, Vol. 22, pp. 53 – 67. ISSN 0100-7386. doi: 10.1590/S0100-73862000000100005.

Wilcox, D.C. *et al.*, 1993. *Turbulence modeling for CFD*, Vol. 2. DCW industries La Canada, CA.

7. RESPONSIBILITY NOTICE

The authors are the only responsible for the printed material included in this paper.